Proceedings Paper:
Tallents, G. J. orcid.org/0000-0002-1409-105X, Wilson, Sarah, Aslanyan, V. et al. (4 more authors) (2018) The Creation of Radiation Dominated Plasmas Using Laboratory X-Ray Lasers. In: X-Ray Lasers 2016 - Proceedings of the 15th International Conference on X-Ray Lasers. 15th International Conference on X-Ray Lasers, ICXRL 2016, 22-27 May 2016 Springer Proceedings in Physics . Springer Science and Business Media, LLC , JPN , pp. 37-43.

https://doi.org/10.1007/978-3-319-73025-7_6

The creation of radiation dominated plasmas using laboratory X-ray lasers

G J Tallents[1], S Wilson[1], V Aslanyan[1], A West[1], A K Rossall[1], C S Menoni[2] and J J Rocca[2]

[1]York Plasma Institute, Department of Physics, University of York, York YO10 5DD, U.K.
[2]Center for Extreme Ultraviolet Science and Technology and Department of Electrical and Computer Engineering, Colorado State University, Fort Collins, Colorado 80523, U.S.A.

Abstract. When short wavelength extreme ultra-violet (EUV) and x-ray laser radiation is focused onto solid targets, narrow deep features are ablated and a dense, low temperature plasma is formed. We examine the radiation dominated plasma formed by 46.9 nm laser radiation focused onto solids and show that ionization can be significantly modified by electron degeneracy effects. Some experimental and theoretical considerations for investigating the interaction of capillary discharge lasers operating at 46.9 nm with solid and gas targets are presented.

1 Introduction

Extreme ultra-violet (EUV) and x-ray lasers can be used to generate strongly coupled plasmas and 'warm dense' matter [1]. Targets irradiated by EUV and x-ray lasers are heated by direct photoionization as well as inverse bremsstrahlung. With EUV and x-ray lasers, lower temperature and higher particle density plasmas are produced than can be created by optical laser irradiation. With optical laser-produced plasmas, an expanding plume of plasma only allows absorption by inverse bremsstrahlung where the electron density drops below a critical value ($\simeq 10^{21}/\lambda^2$ $\mu m^{-2} cm^{-3}$, where λ is the laser wavelength in units of microns). By reducing the wavelength into the EUV to x-ray region, the critical electron density is greater than solid electron densities and the laser photon energy E_p becomes sufficient to directly photo-ionize elemental components (ionization energy E_i), transferring energy ($E_p - E_i$) to the ejected electron. As the critical electron density is higher than solid, the laser is able to penetrate any expanding plasma plume and heat solid material directly throughout the duration of a laser pulse. A large depth of plasma is heated at high density to moderate (a few eV) temperatures.

We explore in this paper the potential for creating narrow and deep features by EUV laser ablation of solids [2], and also for using the plasma created by

EUV lasers as sources for warm dense matter studies. Narrow feature can be ablated due to the short wavelength λ allowing focusing to a diameter of approximately $f\lambda$, where f is the f-number of the focusing optic. Our calculations show that the ionization of plasma can be affected by free electron degeneracy effects with overlap to the plasma conditions found in inertial fusion, where degenerate plasma is created during x-ray driven compression of material. The use of a capillary laser [3,4] operating at 46.9 nm in producing high density degenerate plasma is explored.

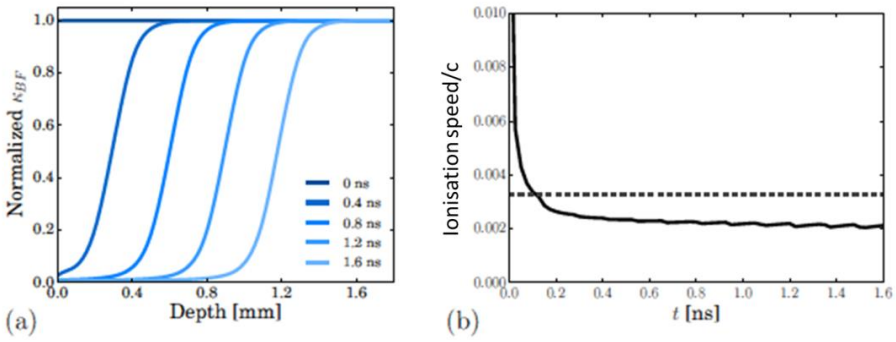

Fig. 1 **(a)** The normalised photoionization absorption coefficient of helium at atmospheric pressure during irradiation by a laser pulse with a flat temporal profile and photon energy 26.4 eV at irradiance of 10^{10} Wcm^{-2}. **(b)** Simulated speed of propagation of the ionisation wave dx/dt (solid), determined as the point where the normalised absorption coefficient takes a value of 0.5, compared to the value following equation (2) assuming zero particle temperature (dashed).

2 Simple model of EUV interaction in gases

It is possible to simply model EUV laser interaction with gas targets [5] as with low density targets there is a large change in opacity after deposition of a defined quantity of energy per unit volume. The thickness of material heated by EUV or x-ray radiation incident on a target is controlled by the integral of the incident irradiance in time. A rapid drop of opacity associated with the ionisation of the target will progress through the target with time due to photo-ionisation, Auger ionisation and inverse bremsstrahlung heating (the last leading to collisional ionisation). If a thickness Δx of target material is ionised, we can equate the energy per unit area from the incident irradiance I in a time Δt with the energy per unit area which is ionised i.e.

$$I\Delta t = N(E_{ion} + kT)\Delta x \qquad (1)$$

where N represents the number of electrons per unit volume heated to temperature T and E_{ion} is the summation of the average ionisation energy per

electron required to produce an ionisation stage with a sufficiently large ionisation energy that further photo-ionisation is not possible. It is assumed that the ion temperature remains small.

Re-arranging gives an estimate of the velocity of an ionisation wave through the target:

$$v_{ion} = \frac{\Delta x}{\Delta t} = \frac{I}{N(E_{ion} + kT)} . \quad (2)$$

The plasma temperatures achieved can be estimated by relating the energy density absorbed $E_{ion} + kT$ to the temperature and by measuring the speed v_{ion} of the propagation of an ionisation wave (see equation 2). The necessary ionisation energy density E_{ion} can be estimated by calculating the energy density required to ionize the material sufficiently so that the ionization energy becomes greater than the photon energy. Equation (2) is remarkably accurate for EUV interactions in gases. In figure 1, we compare a detailed simulation of the ionisation wave propagation [6] with the analytic expression given by equation (2) for an EUV laser interaction with a gas at atmospheric density.

3 EUV interactions with solid targets

With EUV interactions onto solid targets, the higher density plasma undergoes significant inverse bremsstrahlung absorption as well as photo-ionization so that the model of 'bleaching' after deposition of energy $E_{ion} + kT$ per electron breaks down. Inverse bremsstrahlung causes additional heating raising the value of NkT without a change of the material opacity (see figure 2).

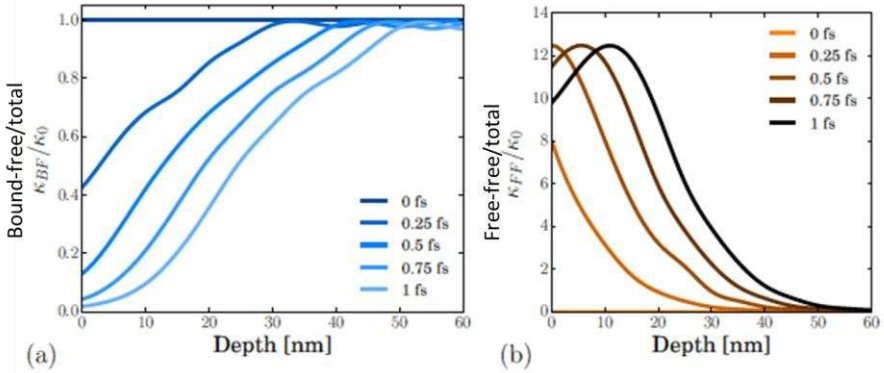

Fig. 2 The contribution to the absorption coefficient due to (a) photo-ionization and (b) inverse bremsstrahlung for solid density carbon irradiated by photons at irradiance 10^{14} Wcm^{-2} and photon energy 26.4 eV at times indicated. The absorption coefficients are normalised to the photo-ionization coefficient for neutral carbon.

Experiments where a capillary discharge laser is focused onto solid parylene targets have been undertaken and simulated using a 2D fluid code [7]. The agreement between experiment and the simulations in the depth of material ablated in a single shot is good for experiments undertaken with a 1.3 ns duration capillary focused to different fluence values (see figure 3). A small fraction of the EUV laser output was focused with Fresnel zone plate operating at f/4. The depth of the ablated craters was measured post-shot using an electron microscope.

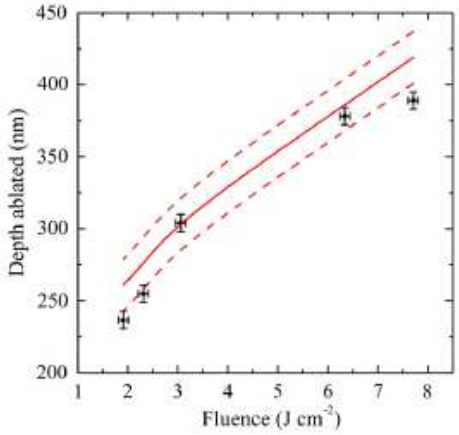

Fig. 3 Comparison between experimental ablated depth measurements (squares) and simulations (solid line) as a function of EUV laser fluence on target. The dashed line indicate the resolution of the Eulerian mesh used in the simulations. Each data point represents the ablation depth for a single shot at the indicated fluence which was determined from the area of the ablated surface.

At irradiances higher than figure 3 (i.e. > 10^{10} Wcm^{-2}), we found that shock wave or other effects cause additional target damage after the shot. An experiment utilising the full energy of the capillary laser was undertaken with spherical multi-layer mirror focusing and collection optics to measure the transmission of the laser through thin targets of parylene or alumimium (see figure 4). Using spherical multilayer mirrors collecting the full laser beam profile enabled higher irradiances on-target than was possible using Fresnel zone-plate focusing optics. For more details of this experiments, see the paper by Aslanyan et al [8]. Wave optic simulations of the focused laser beam profile including aberation effects due to a 4.7 degree tilt on the focusing and collection mirrors agreed with microscope images of the damaged targets. However, the transmission of the laser through the target was best modelled using our fluid code calculations of the shape of the ablated laser hole to evaluate the transmitted image including diffraction. Any cold target material is highly opaque to the EUV lasers, so the transmitted image is simply a sum of the diffracted images once ablation through the target thickness has

occurred at some place. A sample transmission image and the simulation of this transmission is shown in figure 4. The agreement of the experimental and simulated images in figure 4 is better than if diffraction is assumed to occur through the post-shot hole produced by EUV laser irradiation confirming that additional post-shot damage to the target occurs due to shock waves and other effects.

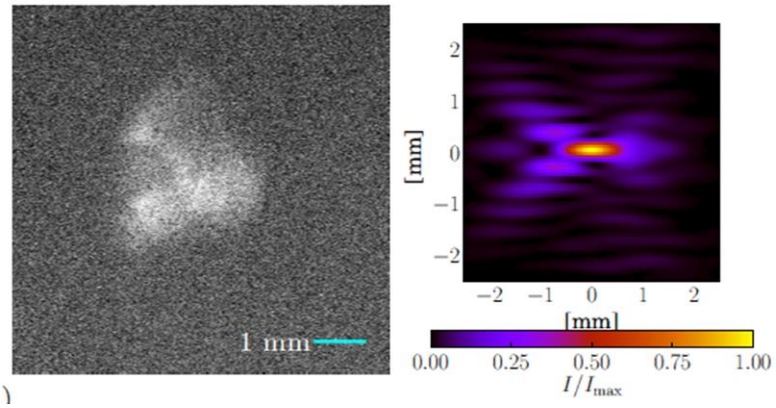

Fig. 4 A measured profile of the EUV laser (left) and a simulated profile (right) transmitted through a parylene target of thickness 1028 nm. The transmitted EUV laser light is collected with a multi-layer mirror which is identically positioned as a multilayer mirror used to focus the EUV laser onto the target. Transmission of EUV light only occurs when the target has been ablated through the total target thickness.

4 Degeneracy effects

Due to the penetration of EUV radiation into solid density material during EUV laser interaction with a solid target, plasma at modest temperatures (< 10eV) and solid density is produced. With only a small amount of ionization, the free electrons can be affected by degeneracy effects. A measure of the degree of free electron degeneracy is given by the reduced chemical potential $\eta = \mu/kT_e$, where μ is the chemical potential and kT_e is the electron temperature [9]. Large negative chemical potential corresponds to conditions where degeneracy effects are unimportant. For densities $\rho > 1$ gcm^{-3} with temperatures $T_e < 3$ eV, degeneracy effects are important for the free electrons and $\eta > 0$.

Calculations show that electron degeneracy significantly reduces collisional rate coefficients for excitation and ionization process due to the reduction of possible free electron quantum states for the colliding electrons [7]. These reductions can modify the ionization and heat capacity of plasma as shown by Aslanyan and Tallents [10]. Steady state calculations of the degree of

ionization of solid density carbon show that in the presence of a significant irradiance (> 10^{14} Wcm^{-2}) of EUV radiation, the degree of ionization is different assuming a Maxwellian distribution of electrons and assuming a Fermi-Dirac distribution (figure 5). At high irradiance, photo-ionization is in balance with three-body recombination. Due to the two free electrons involved in three-body recombination, the rate of this process is much more affected by degeneracy effects than photo-ionization and so the steady state ionization balance is changed due to the degeneracy effects.

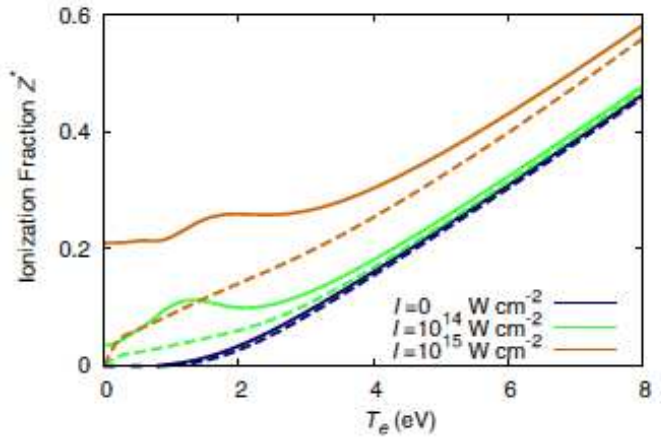

Fig. 5 The steady state ionization Z^* of a carbon plasma at solid density irradiated by EUV photons of energy 50 eV at the indicated irradiance as a function of electron temperature. The free electron distribution is assumed to be Fermi-Dirac (solid curves) or Maxwellian (broken curves).

5 Conclusion

We have shown that when short wavelength extreme ultra-violet (EUV) and x-ray laser radiation is focused onto solid targets, deep features are ablated. A dense, low temperature plasma is formed. We have examined the radiation dominated plasma formed by 46.9 nm laser radiation focused onto solids and have shown that ionization can be significantly modified by electron degeneracy effects. The regimes where electron degeneracy effects are important have been quantified and sample simulations presented showing the effects of free electron degeneracy on plasma ionization under conditions found in solid-density plasmas irradiated by EUV lasers.

References

[1] Berrill, M., Brizuela, Langdon, F. B., Bravo, H., Menoni, C. S. and Rocca, J. J. 'Warm photoionized plasmas created by soft x-ray laser irradiation of solid targets': *J. Opt. Soc. Am.* B **25**, 32, 2008.

[2] Bravo, H., Szapiro, B. T., Wachulak, P. W., Marconi, M. C., Chao, W., Anderson, W. H., Menoni, C. S., and Rocca, J. J.: 'Demonstration of nanomachining with focused extreme ultraviolet laser beams' *IEEE J. Sel. Top. Quantum Electron.* **18**, 443, 2012.

[3] Rocca, J. J., Shlyaptsev, V. N., Tomasel, F. G., Cortazar, O. D., Hartshorn, D., and Chilla, J. L. A.; 'Demonstration of a discharge pumped table-top soft X-ray lasers' *Phys. Rev. Lett.* **73**, 2192, 1994.

[4] Benware, B. R., Macchietto, C. D., Moreno, C. H. and Rocca, J. J.: 'Demonstration of a high average power tabletop soft X-ray laser' *Phys. Rev. Lett.* **81**, 5804, 1998.

[5] Tallents, G. J.,Whittaker, D. S., Wilson, L. A. and Wagenaars, E. 'Heating of high energy density plasmas using EUV and x-ray lasers' *Proc. SPIE* 8140, 81400F, 2011.

[6] Aslanyan, V: *Extreme ultraviolet lasers and their interactions with matter.* PhD thesis 2016 (unpublished).

[7] Rossall, A. K., Aslanyan, V., Tallents, G. J., Kuznetsov, I., Rocca J. J. and Menoni, C. S.: 'Ablation of submicrometer holes using an extreme ultra-violet laser' *Phys. Rev. Appl.* **3**, 064013, 2015.

[8] Aslanyan, V., Kusznetsov, I., Bravo, H., Woolston, M. R., Rossall, A. K., Menoni, C. S., Rocca, J. J. and Tallents, G. J.: 'Ablation and transmission of thin solid targets irradiated by intense extreme ultraviolet laser radiation' *APL Photonics* **1**, 066101, 2016.

[9] Tallents, G. J. 'Free electron degeneracy effects on collisional excitation, ionization , de-excitation and three-body recombination' *HEDP* **20**, 9, 2016.

[10] Aslanyan, V. and Tallents, G. J.: 'Ionization rate coefficients in warm dense plasmas' *Phys. Rev.* E**91**, 063106 2015.